# Dynamic absorption coefficients of chemically amplified resists and nonchemically amplified resists at extreme ultraviolet

Fallica, Roberto; Stowers, Jason; Grenville, Andrew; Frommhold, Andreas; Robinson, Alex; Ekinci, Yasin

*DOI:*
10.1117/1.JMM.15.3.033506

Journal of
Micro/Nanolithography,
MEMS, and MOEMS

Nanolithography.SPIEDigitalLibrary.org

# Dynamic absorption coefficients of chemically amplified resists and nonchemically amplified resists at extreme ultraviolet

Roberto Fallica
Jason K. Stowers
Andrew Grenville
Andreas Frommhold
Alex P. G. Robinson
Yasin Ekinci

SPIE.

Roberto Fallica, Jason K. Stowers, Andrew Grenville, Andreas Frommhold, Alex P. G. Robinson, Yasin Ekinci, "Dynamic absorption coefficients of chemically amplified resists and nonchemically amplified resists at extreme ultraviolet," *J. Micro/Nanolith. MEMS MOEMS* **15**(3), 033506 (2016), doi: 10.1117/1.JMM.15.3.033506.

# Dynamic absorption coefficients of chemically amplified resists and nonchemically amplified resists at extreme ultraviolet

**Roberto Fallica,[a,*] Jason K. Stowers,[b] Andrew Grenville,[b] Andreas Frommhold,[c] Alex P. G. Robinson,[c] and Yasin Ekinci[a]**
[a]Paul Scherrer Institute, 5232 Villigen PSI, Switzerland
[b]Inpria Corporation, 2001 NW Monroe Avenue, Suite 203, Corvallis, Oregon 97330, United States
[c]University of Birmingham, School of Chemical Engineering, Edgbaston, Birmingham B15 2TT, United Kingdom

**Abstract.** The dynamic absorption coefficients of several chemically amplified resists (CAR) and non-CAR extreme ultraviolet (EUV) photoresists are measured experimentally using a specifically developed setup in transmission mode at the x-ray interference lithography beamline of the Swiss Light Source. The absorption coefficient $\alpha$ and the Dill parameters *ABC* were measured with unprecedented accuracy. In general, the $\alpha$ of resists match very closely with the theoretical value calculated from elemental densities and absorption coefficients, whereas exceptions are observed. In addition, through the direct measurements of the absorption coefficients and dose-to-clear values, we introduce a new figure of merit called chemical sensitivity to account for all the postabsorption chemical reaction ongoing in the resist, which also predicts a quantitative clearing volume and clearing radius, due to the photon absorption in the resist. These parameters may help provide deeper insight into the underlying mechanisms of the EUV concepts of clearing volume and clearing radius, which are then defined and quantitatively calculated.  [DOI: 10.1117/1.JMM.15.3.033506]

Keywords: absorption coefficient; Dill parameters; chemical sensitivity; clearing volume; clearing radius.

Paper 16066P received May 4, 2016; accepted for publication Jul. 12, 2016; published online Aug. 8, 2016.

## 1 Introduction

In photolithographic processing, the optimum absorption is determined by the tradeoff between efficiently harvesting the incoming light (high absorption) and the need to maintain a constant intensity throughout the film thickness (low absorption). Photoresists for deep ultraviolet (DUV) and earlier technologies were designed to coat at 200- to 800-nm thickness. These resists were mostly based on diazonaphthoquinone and novolak resins (g-line and i-line) or chemically amplified resists (CAR) compounds (DUV), which yield an absorption coefficient ($\alpha$) ranging from 0.5 to 1 $\mu m^{-1}$.[1,2] At these values of $\alpha$, the intensity of light reaching the bottom of the resist layer is still about 80% of the intensity at the top, which guarantees both an adequate depth clearance and a limited sidewall slope.

On the other hand, extreme ultraviolet (EUV) photoresists are designed to coat at <45-nm thickness and, despite the fact that the absorption coefficient is in the range of few $\mu m^{-1}$, the total optical absorbance can be as low as 10%. The low absorbance has several detrimental consequences on the lithographic process. First, EUV photons are costly and difficult to produce due to the complexity of sources and should be efficiently used. Moreover, the photon density in 13.5 nm wavelength photolithography is about 14 times lower than it is in 193-nm-ArF excimer laser lithography (the dose being the same). As only about 6 photons are incident per $nm^2$ and only 0.03 are absorbed per $nm^3$ in a typical EUV photoresist exposed at 10 $mJ/cm^2$ dose, the photon shot noise becomes more relevant and contributes substantially to line edge roughness.

Resist manufacturers are undertaking several approaches to counterbalance the low absorbance of EUV resists. One approach is to increase the amount of secondary electrons generated per each absorbed photon (i.e., the quantum yield), which depends on the chemical composition of the resist. Another approach, specific to CAR, is to increase the amount of photoacids generated per photon, i.e., the quantum efficiency. These solutions aim at improving the efficiency of each absorbed photon.

A different approach tackles the low absorption by increasing the absorption of the resist by incorporating highly absorbing elements. In general, the linear absorption coefficient of a compound is given by the sum of the atomic absorption cross section $\sigma_a$ of each element, weighted for its relative amount $x_i$ and density $\rho_i$

$$\alpha = \frac{N_A}{\mathrm{MW}} \sum_i x_i \rho_i \sigma_{a_i}, \tag{1}$$

where $N_A$ is the Avogadro number and MW is the molecular weight of the compound. The most promising elements for incorporation in photoresists are the transition metals and semimetals with large atomic numbers whose large *d* orbitals result in the largest interaction with EUV photons, as it can be seen in Fig. 1, where atomic absorption cross section for all elements of atomic number from 1 to 86 is shown.

In recent years, a great technological effort has being put toward the development of resists featuring enhanced absorption. For example, fluorinated polymers have been investigated as the backbone polymers of EUV resists[4–6]

*Address all correspondence to: Roberto Fallica, E-mail: roberto.fallica@psi.ch

1932-5150/2016/$25.00 © 2016 SPIE

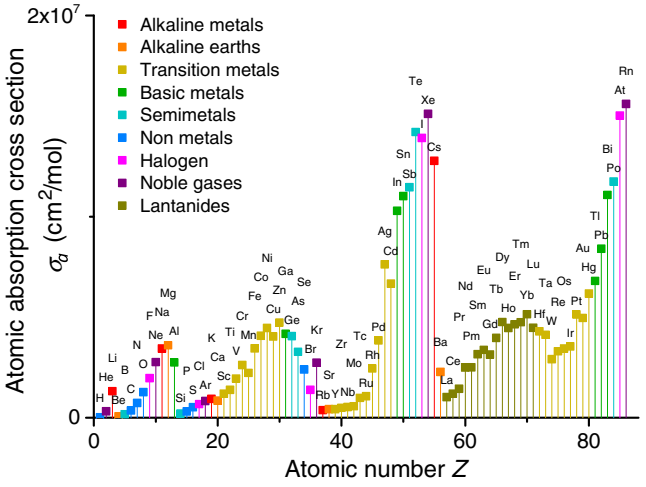


**Fig. 1** Atomic absorption cross sections $\sigma_a$ at EUV of elements with atomic number from $Z = 1$ to 86. Calculated from experimental data.[3]

owing to the large photoabsorption cross section of fluorine atoms. Some fluorine-based resists have been reported to increase the absorption from 5.2 to 7.0 $\mu m^{-1}$, although the change in backbone polymers significantly affects acid generation, acid diffusion, catalytic chain reactions, and dissolution. Other studies claimed fluorinated versions of poly(methyl methacrylate) (PMMA) that could, in principle, provide up to 18 $\mu m^{-1}$ absorbance (up from 3.88 $\mu m^{-1}$ of a conventional FEVS-P1101 resist).[7] The addition of metals is a viable way to synthesize negative-tone photoresists based on organometallic carboxylate compounds of the type [RnM(O2CR′)2], with M = Sn, Te, Bi, Sb.[8] Another method involves the synthesis of photoresists based on nanoparticle/molecular metals. The incorporation of $ZrO_x$ and $TeO_x$ nanoparticles in a CAR has been demonstrated to reduce its transmittance by up to ≈8% depending on the relative amount of oxide compared to the original formulation.[9]

In this work, we measured experimentally the static and the dynamic absorption coefficients of photoresists at EUV (13.5 nm). In addition to the static linear absorption coefficient $\alpha$, the dynamic absorption coefficients are technologically important for accurate chemical and physical modeling of the lithographic process. These coefficients are known as the Dill parameters, or the *ABC* parameters. We chose resists belonging to a broad spectrum of platforms and we discuss these results to determine the chemical sensitivity (CS). The sources of experimental uncertainty are accounted for, thus providing quantitative data with unprecedented accuracy.

## 2 Experimental Methods

### 2.1 *Transmittance Measurement at X-Ray Interference Lithography Beamline*

The x-ray interference lithography (XIL) beamline at Swiss Light Source (SLS) employs synchrotron generated EUV light at 13.5 nm with an average flux in excess of ≈30 mW/cm$^2$. This tool is mainly used for EUV interference lithography[10] and lensless EUV mask imaging. For this study, we made minor additions to the setup enabling us to measure the intensity of the light passing through a sample in transmission mode. The experimental setup is schematically shown in Fig. 2. The beam intensity and shape were set by using a pinhole of 30-$\mu$m diameter. A square open-frame mask ($0.5 \times 0.5$ mm$^2$) was located in front of the sample to crop out the beam tail. The combination of pinhole and openframe resulted in a highly homogeneous beam intensity within the exposed area. Because the membrane itself also absorbs EUV light, we calibrated the net flux $I_0$ through a blank silicon nitride membrane. The transmittance $T_X$ of the thin film is then given by the ratio between the measured photocurrent $I$ and the reference photocurrent $I_0$.

### 2.2 *Linear Absorption Coefficient and Dill Parameters*

As the Beer–Lambert law describes, the transmittance of light through a homogeneous medium is a function of the thickness $d$ and of the linear absorption coefficient $\alpha$:

$$T_X = e^{-\alpha d}. \tag{2}$$

From Eq. 2, the linear absorption coefficient can be calculated as

$$\alpha = -\frac{1}{d} \ln \frac{I(t_0)}{I_0} \ (\mu m^{-1}). \tag{3}$$

In our experimental setup, the current measured from the photodiode was recorded as a function of time, from the beginning ($t = t_0$) and throughout the end of the exposure ($t = t_{exp}$). Here, $t_{exp}$ is the time needed to fully expose the resist, calculated as the ratio between flux (which is constant during the exposure) and the dose-to-clear (DtC), which is also measured with the same tool *a priori*. We thus calculate the bleaching of the photoresist using the definitions of Dill parameters[11] for the bleachable absorption coefficient $A$:

$$A = \frac{1}{d} \ln \frac{I(t_{exp})}{I(t_0)} \ (\mu m^{-1}), \tag{4}$$

the unbleachable absorption coefficient $B$:

$$B = -\frac{1}{d} \ln \frac{I(t_{exp})}{I_0} = \alpha - A \ (\mu m^{-1}), \tag{5}$$

and the exposure rate constant $C$:

$$C = \frac{A + B}{A\Phi[I(0) - I(0)^2/I_0]} \left.\frac{dI}{dt}\right|_{t=0} \left(\frac{cm^2}{mJ}\right). \tag{6}$$

In particular, the Dill $C$ parameter plays a role in the modeling of the reactivity change in a material upon exposure. According to the classic interpretation of CAR in DUV and earlier technology, the solubility change is mediated by the photoacid generator (PAG) concentration $m$ which follows a first-order kinetics ruled by the relationship: $dm/dt = -CI(x, y, z)m$, where $I(x, y, z)$ is the aerial image intensity. As a result, the $C$ parameter accounts for the resist dynamic response. In pre-EUV technology, this parameter reveals the rate of chemical change owing to the formation/disruption of chemical bonding in the material. In EUV technology, where the variation in absorption is uniquely dictated by the amount of mass, the Dill $C$ measures the rate of reaction as a consequence of the mass loss of the resist during exposure.

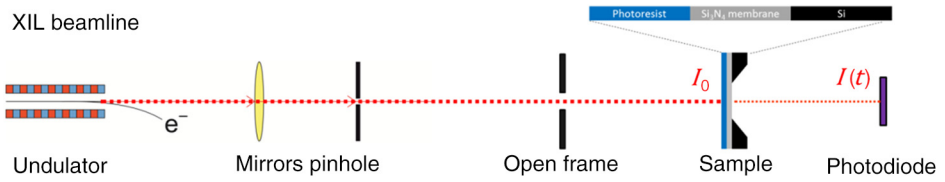


**Fig. 2** Schematic of experimental setup for absorption measurements.

### 2.3 *Sample Preparation and Description*

Silicon nitride membranes (100-nm nominal thickness, $3 \times 3$ mm$^2$) suspended on a silicon frame (280-$\mu$m thick, $9 \times 9$ mm$^2$) were fabricated by selective KOH etch of silicon wafers. Thin photoresist films were subsequently spun coated on the membranes and processed according to the manufacturer specifications (pretreatment, postapplication bake, underlayer, etc.).

For the sensitivity (dosage curve) measurements, the same resists were also spun coated on bulk silicon wafers, 500-$\mu$m thick, and processed according to the manufacturer specifications.

The sample's description is provided in Table 1. We chose the well-known PMMA and hydrogen silsesquioxane (HSQ) as reference systems. Four chemically amplified EUV-specific photoresists, from an undisclosed manufacturer and labeled here 1, 2, and 3 were analyzed. A modified version of the latter resist, featuring increased sensitizer concentration, was also tested (EUV 3+S). Two materials of metal oxide-based photocondensed resists, nonchemically amplified, containing tin from Inpria Corp. (YABA and a YF) were measured. Finally, we measured two fullerene-based resists and two molecular glasses provided from Irresistible Materials, some of which contained metal.

**Table 1** Samples' description.

| Resist | Manufacturer | Type | C.A. | Metal containing |
|---|---|---|---|---|
| PMMA | Sigma-Aldrich | Organic | Non-CA | N |
| HSQ | Dow | Inorganic | Non-CA | N |
| EUV 1 | Undisclosed | Organic | CA | N |
| EUV 2 | Undisclosed | Organic | CA | N |
| EUV 3 | Undisclosed | Organic | CA | N |
| EUV 3 + S | Undisclosed | Organic | CA | N |
| YABA | Inpria | Metal oxide based | Non-CA | Y (Sn) |
| YF | Inpria | Metal oxide based | Non-CA | Y (Sn) |
| xMT-213 | IM | Organic | CA | N |
| PBPM | IM | Organic | Non-CA | Y |
| ML356 | IM | Organic | Non-CA | Y |
| HB1-213 | IM | Organic | CA | Y |

### 2.4 *Spectroscopic Ellipsometry*

The accurate measurement of the thickness of a resist coated on a suspended membrane is challenging and it is a major source of uncertainty in the estimation of $\alpha$. Resist thickness was measured using a Woollam M-2000 spectroscopic ellipsometer with spectral range 250 to 1000 nm and equipped with a focusing probe to reduce the spot size to about 30-$\mu$m diameter. Samples were mounted on an automatic motorized stage and the entire membrane was mapped with a 175-$\mu$m step grid. The spot for the ellipsometer was a 92 $\mu$m $\times$ 42 $\mu$m oval. The ellipsometric data were modeled as two layers, for the SiN membrane a B-spline dispersion model seeded with $Si_3N_4$ material properties and for the resist a Cauchy model. Initial material fits were generated from the silicon frame surrounding the suspended membrane. Neither additional layers nor interfacial were needed to obtain a good fitting of the thickness. This approach greatly reduces the uncertainty in the $\alpha$, using a combination of optical inspection and spectroscopic ellipsometry to estimate $d$ in the proximity of the exposed area.

### 2.5 *Estimation of Uncertainty*

The uncertainty in the measurement of $\alpha$ arises from three sources. The first is the uncertainty in the measurement of the resist thickness ($\sigma_d$), due to the nonuniformity of the coating. The second is the uncertainty in the thickness of the silicon nitride membrane, due to the KOH etch variability, which affects the value of the reference photocurrent ($\sigma_{I0}$). The third is the uncertainty in the measured photocurrent from the photodiode ($\sigma_I$). The standard deviation of $\alpha$ is then given by the well-known equation for error propagation and replacing the due quantities:

$$\sigma_\alpha = \sqrt{\left(\frac{\partial\alpha}{\partial d}\right)^2\sigma_d^2 + \left(\frac{\partial\alpha}{\partial I_0}\right)^2\sigma_{I_0}^2 + \left(\frac{\partial\alpha}{\partial I(t)}\right)^2\sigma_{I(t)}^2}$$

$$\cong \sqrt{\left(\frac{\partial\alpha}{\partial d}\right)^2\sigma_d^2 + \left(\frac{\partial\alpha}{\partial I_0}\right)^2\sigma_{I_0}^2} = \sqrt{\alpha^2\frac{\sigma_d^2}{d^2} + \frac{1}{d^2}\frac{\sigma_{I_0}^2}{I_0^2}}. \quad (7)$$

From experimental data, the fluctuations in measured photocurrent were negligible in comparison to the other terms of Eq. (7) and were not taken into account.

## 3 Results and Discussion

### 3.1 *Linear Absorption Coefficient $\alpha$*

The measured transmittance of all samples is plotted in Fig. 3 as a function of resist thickness $d$. Resists that were coated at

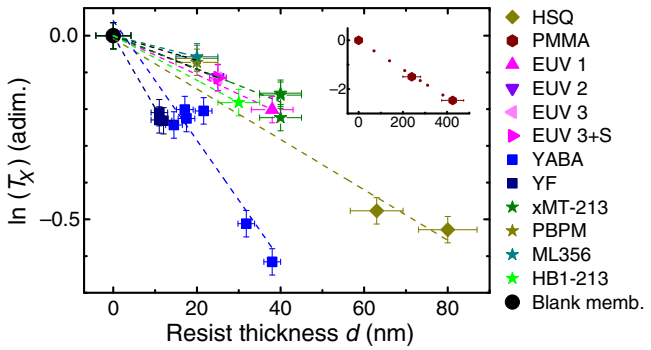


**Fig. 3** Logarithm of measured transmittance as a function of resist film thickness. For each measurement point, the *X*-axis error bar indicates the uncertainty in the thickness measurement $\sigma_d$ and the *Y*-axis error bar indicates the uncertainty in the transmittance $\sigma_{Io}$. The dashed lines are the linear fit to the data. The slope of the fit is the linear absorption coefficient $\alpha$. Inset: measured data for PMMA.

different thicknesses showed a linear relation between the logarithm of transmittance and $d$, which indicates a homogeneous optical absorption through the medium. The linear absorption coefficient $\alpha$ can thus be determined as the slope of the linear fit to the data. The linear fit is weighted by the *X*-axis error bar, which indicates the uncertainty in the thickness measurement $\sigma_d$, and by the *Y*-axis error bar, which indicates the uncertainty in the transmittance $\sigma_{Io}$. (For those resists spin coated at only one thickness, we consider the line through the origin.)

The measured $\alpha$ is summarized for all samples in Fig. 4; the error bar is calculated from the error-weighted linear fit of the $T_X$ versus thickness plot.

The photoresists based on the tin oxide (YABA and YF) showed the highest absorption values, while all the other resist platforms are three to four times lower. A previous theoretical study predicted that resists based on polymeric backbones only achieve $\alpha$ values in the 3 to 5 $\mu m^{-1}$ range,[12] as a consequence of the chemical composition, where only C and O atoms contribute to the absorption. Our result for PMMA is in good agreement with the previous experimental studies, which reported that its EUV absorption is between ≈5,[13] and 4.8 $\mu m^{-1}$.[12] Note that the CAR with added sensitizer (EUV 3 + S) had the same absorption coefficient as its

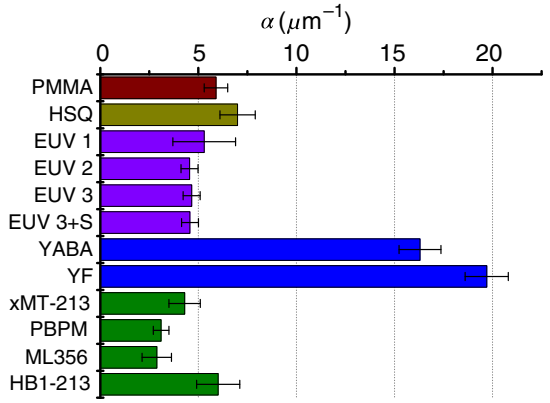


**Fig. 4** Measured linear absorption coefficient $\alpha$. All polymer-based resists have approximately the same value, while the tin oxide-based resists (YABA and YF) have a remarkably higher $\alpha$.

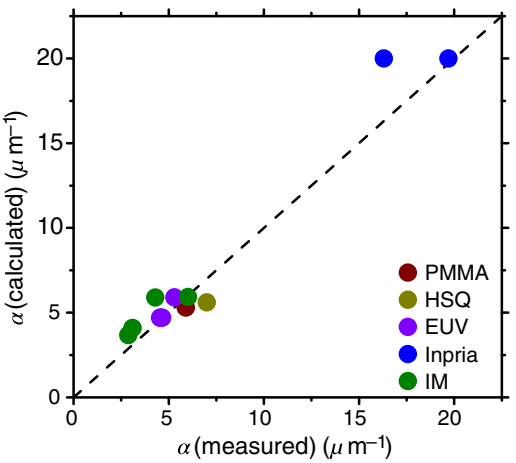


**Fig. 5** Comparison between experimental and theoretical absorption coefficient for all resists in this work. The dash line indicates the exact match.

baseline formulation (EUV 3). Other resists with added metal elements also showed higher absorption, 6 $\mu m^{-1}$ (HB1-213), than that of conventional CAR. We conclude that the absorption increases most remarkably only in metal-added nonpolymer-based resists. Our values are in agreement with those reported on some typical polymer backbones for EUV, between 2.5 and 5.2 $\mu m^{-1}$ measured using the grazing incidence angle method.[14]

To validate our results, we calculated the theoretical absorption coefficient of these resists using the online database of x-ray interactions,[15] based on tabulated data of x-ray absorption published previously.[3] The chemical composition and density used were for PMMA: $C_5O_2H_8$, molecular weight 950,000, dilution 1%, density 1.2 $g/cm^3$; for HSQ: $Si_8O_{12}H_8$, density 1.4 $g/cm^3$; for proprietary materials, values provided by the manufacturer. The comparison between our experimental data and the calculated data shows a close match between the two (Fig. 5).

### 3.2 *Dill Parameters*

The measured Dill parameters (also known as the *ABC* parameters) are of interest for lithographic modeling. We summarized these results in Fig. 6.

For all resists investigated in this work, and in general for EUV resists, the bleachable coefficient $A$ was found to be positive and much smaller than $\alpha$. The Dill parameter $A$ can also indicate a change in the resist thickness during exposure. As a result of being $A \ll \alpha$, the unbleachable coefficient $B \approx \alpha$. This behavior is notably different to that of i-line and g-line resists, which have $A \gg B$.[1]

The Dill parameter $C$ is proportional to the rate of bleaching at $t = 0$, and is an empirical indicator of the rate of reaction of the resist at the beginning of exposure caused by, among other things, deprotection reactions and mass loss due to outgassing. It was found that the CAR with added sensitizer (EUV 3 + S) yielded a significantly higher reaction rate than its baseline counterpart (EUV 3). In a previous study, other researchers found $C$ parameter values of 0.04 $cm^2/mJ$ for an anion-bound polymer bound CAR using the film thickness loss curves method.[16] Another study by Fourier transform infrared spectroscopy gave a reaction rate of $0.0409 \pm 0.0023$ $cm^2/mJ$ for another undisclosed

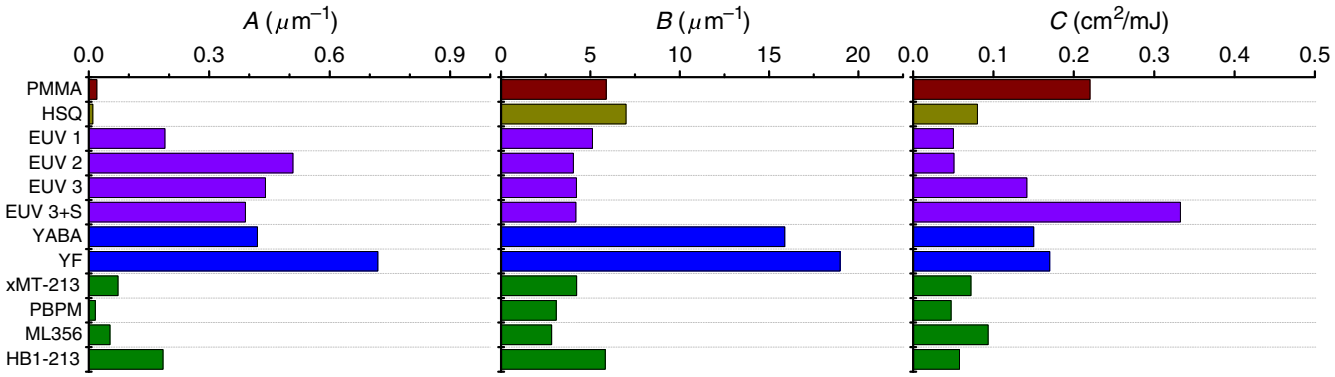


**Fig. 6** Summary of the measured Dill parameters: bleachable coefficient *A*, unbleachable coefficient *B*, and exposure rate constant *C* of resists investigated in this work.

CAR,[17] in good agreement with our result. Other methods reported $C$ in the range of 0.037 to 0.055 $\mathrm{cm}^2/\mathrm{mJ}$.[18–20] In comparison to the previous technological platforms, the Dill $C$ parameter is higher in EUV than it was in UV lithography ($0.022 \approx 0.008\ \mathrm{cm}^2/\mathrm{mJ}$)[1] and in DUV lithography ($0.005\ \mathrm{cm}^2/\mathrm{mJ}$).[2]

### 3.3 *Chemical Sensitivity*

In light of the new understanding of the absorption coefficient $\alpha$, we introduce here a new figure of merit. First, we observe that the lithographic sensitivity of a resist is proportional to the reciprocal of its DtC (or dose to gel):

$$\mathrm{LithoSens} = \frac{1}{\mathrm{DtC}}. \tag{8}$$

Furthermore, we observe that the lithographic sensitivity is proportional to the product of the amount of absorbed photons (via the absorption coefficient) and the combination of quantum efficiency, quantum yield, chemical amplification, and so on (i.e., all chemical reactions which take place after a photon is absorbed):

$$\mathrm{LithoSens} = \alpha \times \sum(\mathrm{QE}, \mathrm{QY}, \mathrm{CA}, \mathrm{etc.}). \tag{9}$$

By rearranging Eqs. (8) and (9), we define chemical sensitivity the quantity:

$$\mathrm{CS} = \frac{1}{\alpha \times \mathrm{DtC}}. \tag{10}$$

CS accounts for the contribution that all secondary chemical reactions make to the overall lithographic sensitivity. Because $\alpha$ is expressed in $\mu\mathrm{m}^{-1}$ and DtC is expressed in $\mathrm{mJ}/\mathrm{cm}^2$, CS is in units of volume per energy ($\mathrm{m}^3/\mathrm{J}$) or, more intuitively, in cubic nanometers per unit energy of an EUV photon ($\mathrm{nm}^3/E_{\mathrm{ph}}$). In this interpretation, the CS indicates the volume of photoresist that is cleared by a single absorbed EUV photon. CS is larger when each absorbed photon triggers a more significant amount of secondary chemical reactions which clear (or condense) a larger resist volume. As it rules out the absorption and the thickness of a material, the CS can be compared across different resist platforms. It aggregates several formulation features into a single parameter of resist reactivity. For instance, in non-CAR, the CS summarizes the effect of cross-linking/condensation quantum efficiency that, coupled with the process conditions, sets a threshold to the sensitivity of the material. In CAR, the CS additionally accounts for the photoacid generation quantum efficiency and the chemical amplification (balance between quencher and diffusion statistics). In addition, the secondary electron yield also affects the CS as a consequence of the amount of secondary electrons generated by the absorption.

The CS was calculated using Eq. (10) from measured $\alpha$ and DtC (from contrast curves) for all these resists and the results are shown in Fig. 7. All CAR have CS of several tens of cubic nanometers per photon energy: most of their lithographic sensitivity is caused by a high CS. On the opposite end, all non-CAR have CS below 10 $\mathrm{nm}^3/E_{\mathrm{ph}}$, regardless of any other feature. In agreement with our reasoning, we notice that the CS increases when a sensitizer is added to a CAR (EUV 3 + S) in comparison to the same baseline formulation (EUV 3). The xMT and HB1 materials are chemically amplified but fall in between the two cases given. (As for the PBPM and the ML356 materials, the DtC was not available.)

Higher CS is on one hand desirable to increase the lithographic sensitivity, but on the other hand it sets an ultimate limit to the maximum resolution at which a resist can be patterned. To clarify this, let us consider the sphere of a resist having the volume equal to CS; its radius (clearing radius) indicates the width of the clearing triggered by an absorbed photon and its secondary reactions. The calculated clearing radii for all resists are shown in Fig. 8.

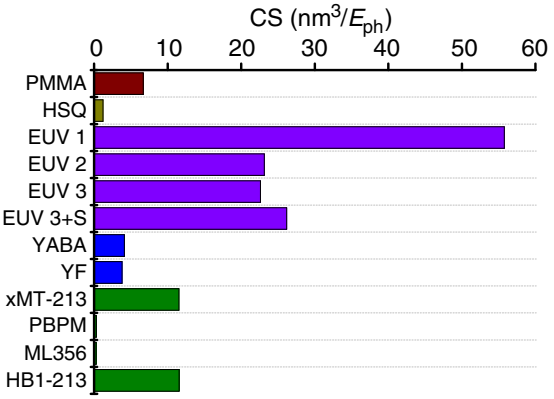


**Fig. 7** CS of resists, calculated from measured $\alpha$ and dose-to-clear values as described in Eq. (10).

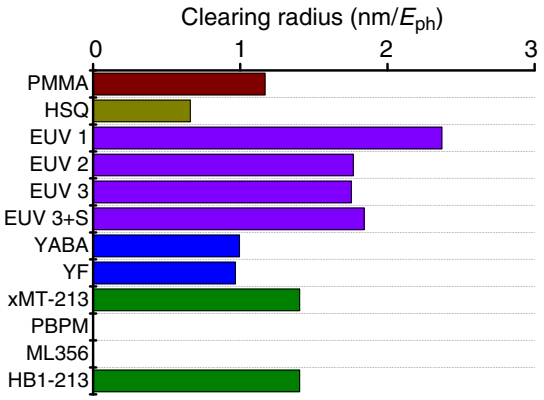


**Fig. 8** Clearing radius of the sphere of volume equal to CS, for each resist.

The definition of clearing volume is based on the minimum volume pixel (voxel) of resist that is cleared by a single absorbed photon. This volume represents the granularity of the resist, thus it can be interpreted as the ultimate resolution limit for a material. It is a consequence of the resist blur (secondary electron blur + acid diffusion blur). For the reasons discussed, the clearing radius is obviously larger in CARs than it is in non-CARs. In the former, the spatial range is in fact increased due to the acid diffusion. In the latter, the radius is only caused by the secondary electron blur (SEB). In this regard, the clearing radius is an indication of the total resist blur. This interpretation agrees with previous theoretical and experimental studies that reported an SEB range of $\approx$2.5 nm[21,22] and an acid diffusion blur $\geq$5 nm.[16,21,22] It should be pointed out that the actual resolution limit of a patterned resist is considerably higher than the resist blur. As a matter of fact, the patterning resolution of a resist is limited by the aerial image log slope, the flare, the photon shot noise, the quencher/PAG statistics (for chemically amplified), the minimum condensation threshold (for negative tone resists), the radius of gyration of a polymer, and other mechanical properties (pattern collapse, substrate adhesion, etc.). All of these nonidealities are not accounted for in the clearing volume, which only represents an ultimate resolution limit.

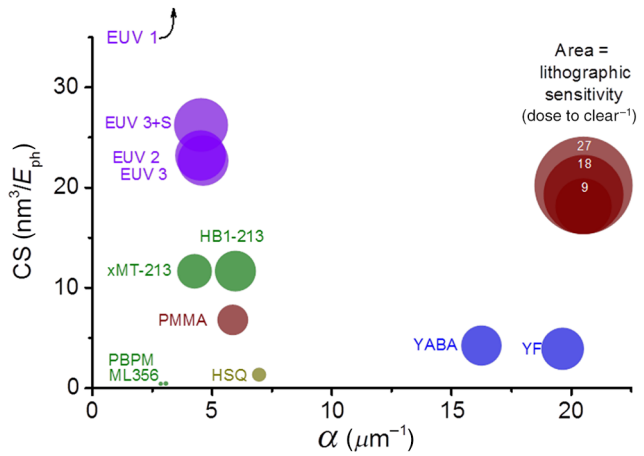


**Fig. 9** Location of resist according to the absorption $\alpha$ and CS. The area of the bubbles is proportional to the total lithographic sensitivity.

The measured $\alpha$ and the newly introduced CS make it possible to draw some conclusions. Figure 9 shows the resist map where each of the samples is now located according to its $\alpha$ and CS. The area of each sample is proportional to the total lithographic sensitivity. The map shows how different resist platforms are being designed to improve the absorption or enhance the CS. The only resist in this work which combines these two approaches is HB1-213. Although higher absorption and higher CS bring the advantage of a higher lithographic sensitivity, there are also drawbacks. On one hand, increasing the former leads to a nonuniform absorption throughout the resist thickness, while increasing the latter reduces the resolution. In other words, these resists are still limited by the RLS tradeoff.

## 4 Conclusions

We developed a methodology for the measurement of the absorption coefficient $\alpha$ and Dill parameters of photoresists at EUV. Our results are consistent with those reported previously for PMMA, HSQ, and with theoretical estimation. Metal oxide-based resists absorb up to 4× more photons than polymer-based resists. In all resists studied in this work, the bleachable $A$ coefficient is positive but is much smaller than the nonbleachable coefficient $B$.

Using our insight of the absorption and total sensitivity, we introduced a new figure of merit, which makes it possible to quantify the efficiency of postabsorption reactions to the total sensitivity of a material. This CS is significantly higher in CARs than in non-CARs. Finally, our methodology provides insight on the two approaches toward higher lithographic sensitivity in EUV photoresists.

### *Acknowledgments*

The authors are grateful to Irresistible Materials Ltd., for sample preparation and fruitful discussion, and to Markus Kropf (PSI) for technical support. Part of this work has been carried out at SLS. One of the authors (R.F.) wishes to acknowledge Inpria Corp. for financial support.

### *References*

1. MicroChemicals, "Optical properties of photoresists," 2013, Application Note, www.microchemicals.com/downloads/application_notes.html (5 February 2016).
2. Y.-S. Sohn, H.-K. Oh, and I. An, "Parameter extraction for 193 nm chemically amplified resist from refractive index change," *J. Vac. Sci. Technol. B* **19**(6), 2077–2081 (2001).
3. B. L. Henke, E. M. Gullikson, and J. C. Davis, "X-ray interactions: photoabsorption, scattering, transmission, and reflection at E = 50 – 30000 eV, Z = 1 – 92," *At. Data Nucl. Data Tables* **54**(2), 181–342 (1993).
4. M. D. Christianson et al., "High absorbing resists based on trifluoromethacrylate-vinyl ether copolymers for EUV lithography," *Proc. SPIE* **8682**, 868216 (2013).
5. Y.-J. Kwark et al., "Absorbance measurement of polymers at extreme ultraviolet wavelength: correlation between experimental and theoretical calculations," *J. Vac. Sci. Technol. B* **24**, 1822 (2006).
6. A. Sekiguchi et al., "Study of Dill's B parameter measurement of EUV resist," *Proc. SPIE* **9422**, 94222L (2015).
7. R. Gronheid et al., "EUV resist requirements: absorbance and acid yield," *Proc. SPIE* **7273**, 727332 (2009).
8. J. Passarelli et al., "High-sensitivity molecular organometallic resist for EUV (MORE)," *Proc. SPIE* **9425**, 94250T (2015).
9. A. Sekiguchi et al., "A study of EUV resist sensitivity by using metal materials," in *Proceeding P-RE-09 of the Int. Symp. on EUV Lithography.*
10. N. Mojarad, J. Gobrecht, and Y. Ekinci, "Beyond EUV lithography: a comparative study of efficient photoresists' performance," *Sci. Rep.* **5**, 9235 (2015).
11. F. H. Dill et al., "Characterization of positive photoresist," *IEEE Trans. Electron Dev.* **ED-22**, 445–452 (1975).

12. N. N. Matsuzawa et al., "Theoretical estimation of absorption coefficient of various polymers at 13 nm," *Microelectron. Eng.* **53**, 671–674 (2000).
13. G. D. Kubiak et al., "Characterization of chemically amplified resists for soft x-ray projection lithography," *J. Vac. Sci. Technol. B* **10**, 2593 (1992).
14. Y.-J. Kwark et al., "Absorbance measurement of polymers at extreme ultraviolet wavelength: correlation between experimental and theoretical calculations," *J. Vac. Sci. Technol. B* **24**(4), 1822–1826 (2006).
15. E. Gullikson, "The Center for X-Ray Optics, L. B. N. L. s.," http://henke.lbl.gov/optical_constants/ (1 February 2016).
16. R. Gronheid et al., "Resolution-linewidth roughness-sensitivity performance tradeoffs for an extreme ultraviolet polymer bound photo-acid generator resist," *J. Micro/Nanolith. MEMS MOEMS* **10**(1), 013017 (2011).
17. C.-T. Lee et al., "A simple method for measurement of photoacid generator photoreaction kinetics in formulated, chemically amplified photoresist films," *Electrochem. Solid-State Lett.* **10**(9), H273–H277 (2007).
18. C. R. Szmanda et al., "Measuring acid generation efficiency in chemically amplified resists with all three beams," *J. Vac. Sci. Technol. B* **17**(6), 3356–3361 (1999).
19. A. R. Pawloski, C. R. Szmanda, and P. F. Nealey, "Evaluation of the standard addition method to determine rate constants for acid generation in chemically amplified photoresist at 157 nm," *Proc. SPIE* **4345**, 1056–1065 (2001).
20. J. F. Cameron et al., "Comparison of acid-generating efficiencies in 248 and 193-nm photoresists," *Proc. SPIE* **4345**, 106–118 (2001).
21. T. Kozawa and S. Tagawa, "Thermalization distance of electrons generated in poly(4-hydroxystyrene) film containing acid generator upon exposure to extreme ultraviolet radiation," *Jpn. J. Appl. Phys.* **50**, 030209 (2011).
22. J. W. Thackeray et al., "Understanding the role of acid vs. electron blur in EUV resist materials," *J. Photopolym. Sci. Technol.* **23**(5), 631–637 (2010).

Biographies for the authors are not available.